9.1

TURBULENCE DISSIPATION RATE MEASURED BY 915 MHZ WIND PROFILING RADARS COMPARED WITH IN-SITU TOWER AND AIRCRAFT DATA

William J. Shaw*
Pacific Northwest National Laboratory
Richland, Washington

Margaret A. LeMone
National Center for Atmospheric Research
Boulder, Colorado

1. INTRODUCTION

During the last several years Pacific Northwest National Laboratory (PNNL) has been investigating the decay of turbulence in the atmospheric boundary layer during the transition from afternoon convection to evening stable stratification. As part of that study we have worked to extract the dissipation rate of turbulence kinetic energy from a 915 MHz wind profiling radar. Our approach has followed the methods of Gossard et al. (1998) and White et al. (1999) for relating the width of the wind peak in the radar range-gate spectra to dissipation.

Because we are interested in the turbulence decay process, it is important to resolve temporal changes of the turbulence as finely as possible. Ideally, we wish to obtain credible dissipation measurements from individual beam cycles. This requires both accuracy and automation in the algorithm that resolves the profiler Doppler spectral peaks. This motivated our use of the National Center for Atmospheric Research's (NCAR's) Improved Moment Algorithm (NIMA) to extract moments from wind profiler data (Cornman et al. 1998; Morse et al. 2002; Goodrich et al. 2002).

To verify our calculations of dissipation from the profiler, we sought opportunities for intercomparison with dissipation measured by other platforms. As an initial effort, PNNL carried out a brief pilot study by operating a profiler near a sonic anemometer mounted on a tower. As a second comparison, we have used profiler and aircraft data collected during the 1997 Cooperative Atmosphere Surface Exchange Study (CASES-97). In this paper we summarize our calculations of dissipation from the wind profilers, and we compare profiler-derived dissipation measurements with *in situ* measurements from the tower and aircraft.

2. THE OBSERVATIONS

2.1 HMS Tower

The Hanford Meteorological Station (HMS), part of the U.S. Department of Energy's Hanford Site in south-central Washington state, includes among its facilities a 122-m instrumented tower. In April 2000 the 915 MHz wind profiling radar was located approximately 500 m away from this tower. This radar is a four-panel, five-beam phased array system. The beam width is 9º, and the zenith angle of the off-zenith beams is 23.6º. The profiler was operated in a single mode. The vertical resolution was 55 m, and the profiler completed one beam cycle in 4.25 min.

For several days during the month, PNNL operated a sonic anemometer at the 120-m level on this tower, which placed it near the center of the lowest range gate of the profiler. The anemometer sampling rate was 10 s^{-1}.

2.2 CASES-97

CASES-97 (LeMone et al. 2000; Yates et al. 2001) was a field program that was part of a continuing effort to understand the diurnal variation of the boundary layer as influenced by surface processes and to investigate appropriate scaling for precipitation and soil properties. The field campaign used the Atmospheric Boundary Layer Experiments facility (ABLE; Coulter et al. 1998) in the Walnut River watershed in southeastern Kansas. Data from this program were supplied by numerous systems, including wind profilers and aircraft.

The two 915 MHz wind profilers used in this analysis are operated by Argonne National Laboratory as part of the ABLE array. One wind profiler, using a four-panel phased-array antenna, is installed at Whitewater, Kansas. This system is essentially identical to the profiler operated by PNNL on the Hanford Site. The other profiler uses a nine-panel antenna and is installed at Beaumont, Kansas. Because of the larger size of the antenna, the beam width for the Beaumont profiler is 7º in contrast to 9º for the four-panel systems. The profilers operated continuously during the CASES-97 field program.

Two research aircraft, a King Air operated by the University of Wyoming and a Twin Otter operated by the National Oceanic and Atmospheric Administration (NOAA), also participated in the CASES-97 field program. These aircraft flew straight-and-level flight legs at multiple altitudes in the boundary layer for the purpose of measuring profiles of turbulence variables. The legs were typically several tens of kilometers in length. The three wind components were sampled by the King Air at 50 s^{-1}, and the Twin Otter at 40 s^{-1}. The sampling airspeed was 85-90 m s^{-1} for the King Air and 60-65 m s^{-1} for the Twin Otter.

**Corresponding author address:* William J. Shaw, Pacific Northwest National Laboratory, PO Box 999, MS K9-30, Richland, WA 99352. e-mail: will.shaw@pnl.gov.

3. TREATMENT OF THE DATA

3.1 Sonic Anemometer

Dissipation was extracted from the sonic anemometer on the HMS Tower using the inertial subrange of the velocity power density spectra. Spectra were computed from the time series over half-hour intervals after subtraction of a linear trend. We make use of the power-law form of the inertial subrange for a one-dimensional velocity spectrum

$$F_i(k_1) = \alpha_i \varepsilon^{2/3} k_1^{-5/3} \tag{1}$$

where i = 1, 2, or 3 represents the along-wind, cross-wind, or vertical velocity component, α_i is the Kolmogorov constant appropriate to the component, ε is the dissipation rate, and k_1 is wavenumber in the longtitudinal (along-wind) direction. The representation of the spectrum in the frequency domain is

$$F_i(f) = \left(\frac{S}{2\pi}\right)\alpha_i \varepsilon^{2/3} f^{-5/3} \tag{2}$$

where S is the mean wind speed over the half hour. We integrated the individual spectra from 2Hz to 5 Hz (Nyquist frequency), summed the results from each component, used $\alpha_1 = 0.52$ and $\alpha_2 = \alpha_3 = (4/3)\alpha_1$, and solved for the dissipation rate.

3.2 Aircraft

Processing data from the aircraft was similar to the method for the sonic anemometer except that we were able to use a decade or more of the power spectrum and only dissipations based on the longitudinal velocity u were used. In this case S is the mean true air speed for a flight leg, and k_1 is wavenumber along the flight path. Dissipation rate was calculated for each straight-and-level flight leg.

Comparing the aircraft and profiler data was not straightforward, because the aircraft legs were flown in multiple locations and not necessarily near a profiler, although flight legs tended to be nearer to Beaumont than to Whitewater. To accomplish the comparison, therefore, we grouped legs by altitude, creating a single average for a flight day by altitude bin. Using the average time for each group, we created an average dissipation rate from each profiler for an hour centered on the average aircraft time for a given altitude. The intent is that the averaging will minimize differences due to space and time variations of turbulence in the boundary layer.

3.3 Wind Profilers

Because the practical extraction of dissipation rate from profilers is a relatively new development, we provide a more detailed outline of that process. Profiler-derived dissipation rate depends on the broadening of the Doppler spectral peaks by isotropic eddies in the scattering volume illuminated by the radar pulses. The width of the spectral peaks represents the distribution of velocity about the mean radial velocity of the scattering volume. The velocity variance of this distribution is a combination of effects of the isotropic eddies and other non-turbulent effects, such as mean wind shear across the beam, mean wind blowing transverse to a beam of finite width, and the effect of low-frequency variations in the wind during the dwell time for each beam. These effects may be summarized, following White et al. (1999), with

$$\sigma_t^2 = \sigma_s^2 + \sigma_a^2 + \sigma_{11}^2 \tag{3}$$

where σ_t^2 is the total variance measured in the Doppler spectral peak, σ_s^2 is the contribution from shear across the radar beam, σ_a^2 is a contribution depending on antenna properties (which is significant only for scanning radars), and σ_{11}^2 is the radial velocity variance in the sampling volume. For σ_s^2 we have followed Gosssard et al. (1998) in using

$$\sigma_s^2 = \frac{V_T^2 \theta_a^2}{2\ln 4} \tag{4}$$

where V_T is the wind velocity transverse to the beam and θ_a is the radar beam half-width in radians. The contribution σ_{11}^2 consists of

$$\sigma_{11}^2 = \sigma_{\text{point}}^2 - \sigma_{\text{vol}}^2 + \sigma_T^2 \tag{5}$$

where σ_{point}^2 is radial velocity variance that would be measured by a point sensor, σ_{vol}^2 is variance of volume-averaged radial wind, and σ_T^2 is the variance resulting from low-frequency variations in the wind during a beam's dwell time T. White et al. (1999) have modified an expression for σ_{11}^2 originally derived by Frisch and Clifford (1974) in order to include the effect of σ_T^2. Their result is

$$\sigma_{11}^2 = \frac{\alpha \varepsilon^{2/3}}{4\pi} I \tag{6}$$

where $\alpha \cong 1.6$ is a Kolmogorov constant, and I is an intractable triple integral. White et al. showed that I could be well represented in spherical coordinates by

$$I = 12\Gamma\left(\frac{2}{3}\right)\int_0^{\pi/2} d\phi \int_0^{\pi/2} d\theta \times \\ \sin^3\theta \left(b^2\cos^2\theta + a^2\sin^2\theta + \frac{L^2}{12}\sin^2\theta\cos^2\phi\right)^{1/3} \tag{7}$$

which can be evaluated numerically. (We used the function "dblquad" in the commercial software package MATLAB.) The constants a and b are related to beam geometry (White 1997), with

$$a = \frac{R\theta_a}{\sqrt{2\ln 2}} \quad \text{and} \quad b = 0.3\Delta R$$

where ΔR is range gate resolution. $L = \overline{U}T$, where $\overline{U}$ is mean wind speed at a particular range gate, and T is the dwell time. Eqn. 3, after correcting for the shear term (4), yields σ_{11}^2. This in turn yields ε from (6) after evaluating *I* numerically. This procedure, mapped by Gossard et al. (1998) and White et al. (1999), has also recently been used by Jacoby-Koaly et al. (2002). On the occasions where the subtraction of σ_s^2 yielded a negative value, we neglected the estimate, assuming that the dissipation was too small to be extracted from profiler noise. This procedure was also followed by Jacoby-Koaly et al.

4. COMPARISON

4.1 Profiler—HMS Tower

Fig. 1 shows a diurnal cycle of dissipation rate from the lowest range gate of the profiler and from the sonic anemometer, which, at 120 m, was nearly centered in this range gate. This figure shows several characteristics of the April 2000 comparison. First, the diurnal cycle of dissipation rate is evident in both time series. In this particular case, both instruments show a very similar pattern of the increase of dissipation rate in the morning to comparable maximum values around midday. On numerous but not all other days (not shown), maximum values of dissipation from the profiler were larger than those from the sonic. Second, the decrease of dissipation rate in the afternoon was more abrupt from the sonic than from the profiler. This was a common feature during the April 2000 measurements. Finally, the nighttime values of dissipation rate were typically much smaller from the sonic than from the wind profiler.

There were encouraging aspects to this comparison, but there were also obvious disagreements between the instruments. The generally larger values of dissipation from the profiler could, of course, result from still-inadequate removal of non-turbulent broadening of the Doppler spectral peaks. Meteorological factors could also contribute, though. For example, at 120 m the sonic anemometer is often within the surface boundary layer, where gradients of dissipation rate are large and non-linear. Because the corresponding profiler range gate extends from 90 m to 150 m above the surface, it is possible that the profiler values are skewed by large values of dissipation below the height of the sonic anemometer. This would seem to be a particular possibility when turbulence is decaying in the afternoon and could explain the earlier drop in dissipation measured by the sonic in Fig. 1. Thus we sought a further comparison between profiler-derived dissipation and airborne measurements well away from the surface.

4.2 Profiler—Aircraft

Fig. 2 shows profiles of dissipation rate derived from the aircraft and profilers for four days during CASES-97. These figures are presented in chronological order. It should be noted that the lowest aircraft flight legs were lower than the lowest profiler range gates. Further, in the King Air data from 20 May, the lower point of the profile occurred after 0000Z, and we had not obtained profiler data from the succeeding day at the time of this writing.

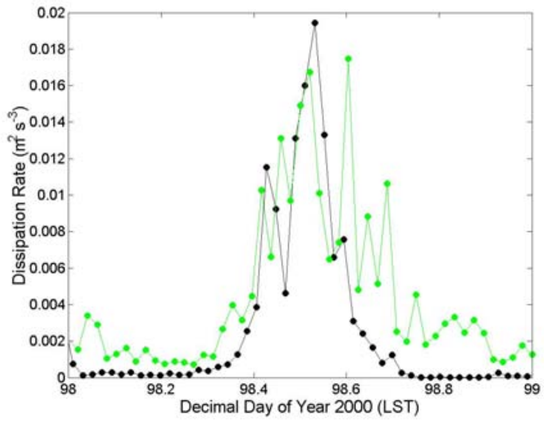

Figure 1. Time series of dissipation rated measured by a sonic anemometer (black) mounted 120 m above the surface and the lowest range gate of a wind profiling radar (green).

There are several features that are common to all of the profiles. First, the qualitative variation of dissipation with height is generally the same in the aircraft and radar profiles. Fig. 2b, in particular, shows that the profilers and the aircraft have the same qualitative structure for dissipation values of the order 10^{-4} m^2 s^{-3}. This provides an indication that the lower bound of measurements from the profilers is small enough to capture the typical range of dissipation within the boundary layer. Second, there is a tendency for the lowest range gates of the profiler to indicate a decrease in dissipation rate. This is contrary to the expected behavior of turbulence in the atmosphere and also at odds with the aircraft data. Finally, despite the qualitative similarities, the profiler values of dissipation are consistently larger that those from the aircraft. Moreover, the dissipation measured by the Whitewater profiler is consistently larger than that from the Beaumont profiler.

Fig. 3 shows the data from the profiles of Fig. 2 expressed as a scatterplot of profiler versus aircraft data. This figure reveals clearly the consistently larger values of dissipation from the profilers. The figure also shows, however, the near proportionality between the profilers and the aircraft. The fitted curves are of the form y=ax. For the Beaumont profiler, a=1.4; for Whitewater, a=2.3. The variances explained by each of the fits are 86% and 84%, respectively.

This last result is rather encouraging because it suggests the problem is not a high noise threshold and that a simple correction factor may be adequate as a last correction to obtain good dissipation values from the profiler. We have not yet determined the reason for this disagreement between the profilers and the aircraft. It is interesting that Jacoby-Koaly et al. (2002) obtained a very similar result, which they attributed to the Hanning

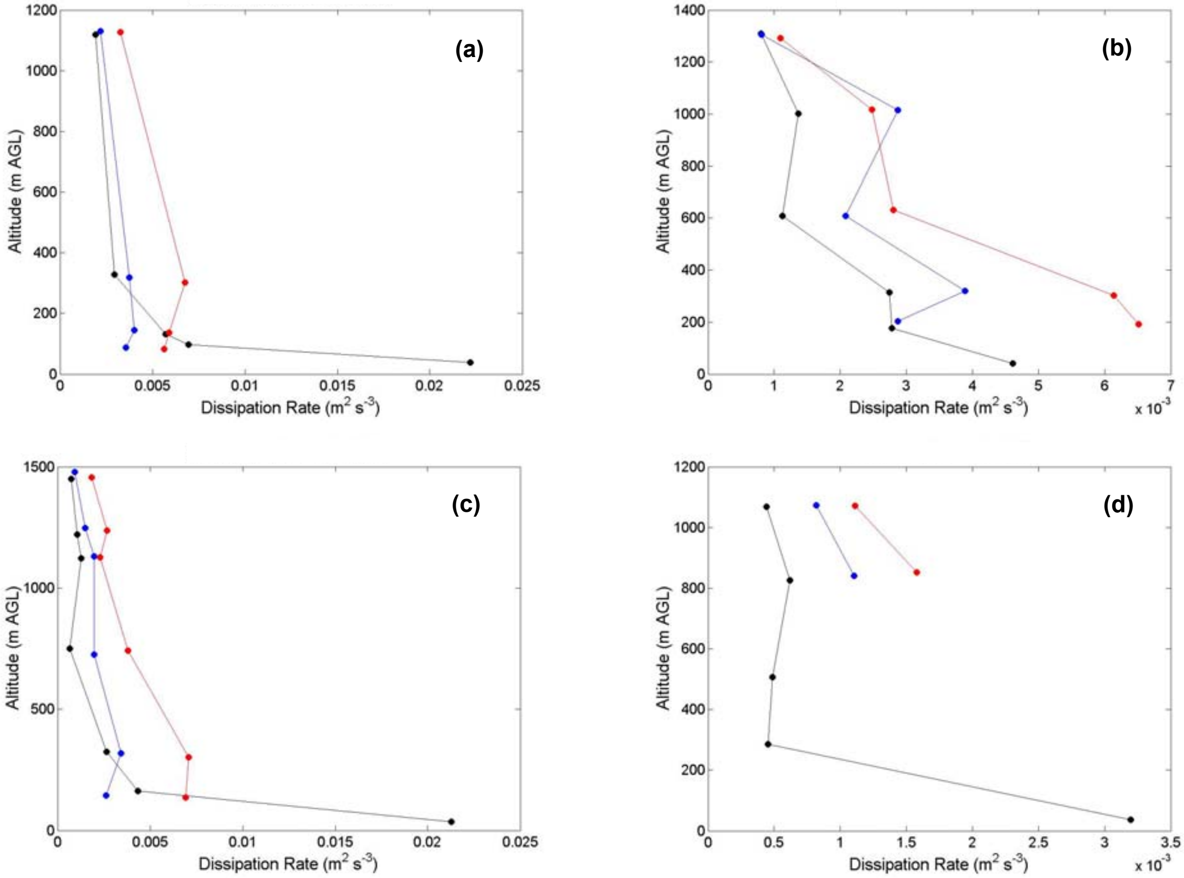

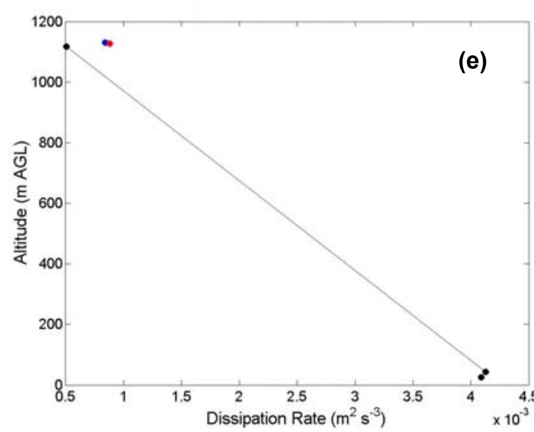

Figure 2. Comparisons between airborne and profiler measurements of dissipation rate during CASES-97. Black symbols are from aircraft; colors are from profilers at Beaumont (blue) and Whitewater, Kansas (red). (a) Comparison with Wyoming King Air on 4 May 1997, (b) with King Air on 10 May, (c) with King Air on 16 May, (d) with King Air on 20 May, and (e) with NOAA Twin Otter on 20 May.

window and other contributions from radar signal processing. Their comparisons with aircraft measurements suggested that this effect was 20% of the raw σ_t. Since dissipation is proportional to the cube of this value, after correction for wind shear broadening the slopes of our best-fit curves suggest that at Whitewater and Beaumont we would need a correction to the standard deviation of 32% and 12%, respectively, which is comparable to Jacoby-Koaly et al.

5. SUMMARY AND CONCLUSIONS

We have used a sonic anemometer mounted on a tall tower and airborne measurements to derive the dissipation rate of turbulence kinetic energy for comparison with observations from several wind profiling radars. We have used the NCAR Improved Moment Algorithm to identify Doppler spectral peaks and calculate their moments. In general, this algorithm provides fairly stable moment estimates from single profiler beam cycles. The comparison with the sonic data allowed us to make inferences regarding the profiler's observations of the diurnal cycle of turbulence. The comparison with aircraft data showed the performance of the profiler over the depth of the mid-to-late-afternoon convective boundary layer.

The PNNL profiler very clearly captured the diurnal cycle of dissipation rate. Values of dissipation calculated from this system, however, tend to be larger than those measured in situ by a sonic anemometer, despite efforts to remove effects of non-turbulent broadening of spectral peaks. Comparisons of ABLE wind profilers that

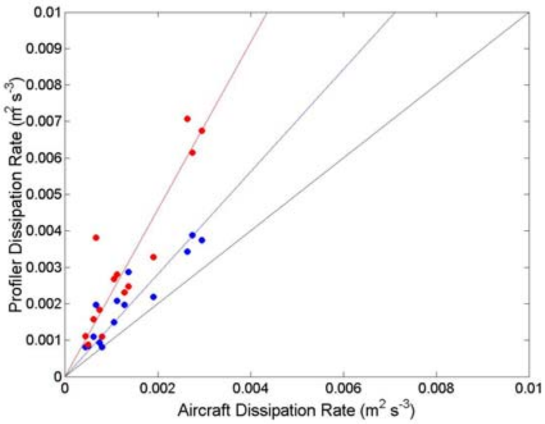

Figure 3. Scatterplot of data from Fig. 2 from all days of the comparison. Black line represents perfect agreement. Colored lines are fits through the origin for data from Beaumont (blue) and Whitewater (red).

operated at Whitewater and Beaumont, Kansas during CASES-97 similarly produced dissipation rates that were larger than those measured by aircraft. Despite the larger magnitudes of dissipation, its qualitative vertical structure in the profiler data was quite similar to that observed by the aircraft. Further, comparisons of boundary-layer-averaged dissipation from the aircraft and the ABLE profilers showed that 85% of the variance in the profiler estimates was explained by the aircraft observations. This suggests that, after removal of established non-turbulent broadening effects, spectral widths from the profilers are driven largely by the small-scale turbulence. Thus, it seems feasible that until the source of this error is understood, a simple correction factor may suffice to obtain good measurements of dissipation rate.

6. ACKNOWLEDGEMENTS

This work was supported by the U.S. Department of Energy (DOE), under the auspices of the Atmospheric Sciences Program of the Office of Biological and Environmental Research. We are grateful to NCAR for providing NIMA to PNNL through a research license and for helpful discussions with Cory Morse of NCAR. This work was performed at Pacific Northwest National Laboratory, which is operated for DOE by the Battelle Memorial Institute under contract DE-AC0676RLO 1830, and at the National Center for Atmospheric Research.

7. REFERENCES

Cornman, L. B., R. K. Goodrich, C. S. Morse, and W. L. Ecklund 1998: A fuzzy logic method for improved moment estimation from Doppler spectra. *J. Atmos. Oceanic Technol.*, **15**, 1287–1305.

Coulter, R. L., G. E. Klazura, B. M. Lesht, J. D. Shannon, D. L. Sisterson, and M. L. Wesely 1998: Using the ABLE facility to observe urbanization effects on planetary boundary layer processes. Preprints, *10th Joint Conference on the Applications of Air Pollution Meteorology*, Phoenix, Arizona. Air and Waste Mgmt. Assoc. and Amer. Meteor. Soc., J76–J79.

Frisch, A. S., and S. F. Clifford 1974: A study of convection capped by a stable layer using Doppler radar and acoustic echo sounders. *J. Atmos.Sci.,* **31**, 1622–1628.

Goodrich, R. K., C. S. Morse, L. B. Cornman, and S. A. Cohn 2002: Horizontal wind and wind confidence algorithm for Doppler wind profilers. *J. Atmos. Oceanic Technol.*, **19**, 257–273.

Gossard, E. E., D. E. Wolfe, K. P. Moran, R. A Paulus, K. D. Anderson, and L. T. Rogers 1998: Measurement of clear-air gradients and turbulence properties with radar wind profilers. *J. Atmos. Oceanic Technol.*, **15**,321–342.

Jacoby-Koaly, S., B. Campistron, S. Bernard, B. Benech, F. Ardhuin-Girard, J. Dessens, E. DuPont, and B. Carissimo 2002: Turbulent dissipation rate in the boundary layer via UHF wind profiler Doppler spectral width measurements. *Bound.-Layer Meteorol.*, **103**, 361–389.

LeMone, M. A., R. L. Grossman, R. L. Coulter, M. L. Wesely, G. E. Klazura, G. S. Poulos, W. Blumen, J. K. Lundquist, R. H. Cuenca, S. F. Kelly, E. A. Brandes, S. P. Oncley, R. T. McMillen, and B. B. Hicks 2000: Land-atmosphere interaction research, early results, and opportunities in the Walnut River watershed in southeast Kansas: CASES and ABLE. *Bull. Am. Meteor. Soc.*, **81**, 757–779.

Morse, C. S., R. K. Goodrich, and L. B. Cornman 2002: The NIMA method for improved moment estimation from Doppler spectra. *J. Atmos. Oceanic Technol.*, **19**, 274–295.

White, A. B., 1997: *Radar Remote Sensing of Scalar and Velocity Microturbulence in the Convective Boundary Layer*. NOAA Tech. Mem. ERL ETL-276, 127 pp.

White, A. B., R. J. Lataitis, and R. S. Lawrence 1999: Space and time filtering of remotely sensed velocity turbulence. *J. Atmos. Oceanic Technol.*, **16**, 1967–1972.

Yates, D. N., F. Chen, M. A. LeMone, R. Qualls, S. P. Oncley, R. L. Grossman, and E. A. Brandes 2001: A cooperative atmosphere–surface exchange study (CASES) dataset for analyzing and parameterizing the effects of land surface heterogeneity on area-averaged surface heat fluxes. *J. Appl. Meteor.*, **40**, 921–937.